Compressor Grating Optimisation using the D scan Technique

Contact: pedro.oliveira@stfc.ac.uk

T. Murphy, P. Oliveira, A.C. Aiken and I. O. Musgrave
Central Laser Facility
STFC Rutherford Appleton Laboratory
Harwell Campus
OXON. OX11 0QX, UK

Abstract

In this contribution we report on our use of the D scan technique to optimise a grating compressor in the Front-End of the Vulcan Laser Facility. We present theoretical and experimental results and demonstrate that this technique is ideal to tune both the incidence angle of the grating and the distance between the gratings. Optimal compression is achieved by eliminating any residual second and third order dispersion, resulting in a shorter compressed pulse.

Introduction

Diffraction gratings are a commonly used method of compressing light which has initially been chirped in time, and are used in variety of experiments, ranging from astrophysics [1], solid state physics [2], quantum physics [3], material processing [4] and two photon effects [5]. These gratings compress such pulses of light by introducing an additional phase to the spectrum of the laser, stretching the pulse in the frequency domain, thus compressing the pulse in the time domain. The overall phase of the pulse is therefore required to determine the relevant parameters of the grating compressor to optimally compress the pulse. Dispersion scans, first established by Miranda et al [6], are a method which allows us to measure such phases. These scans, commonly known as D scans, involve measuring the spectrum of the second harmonic of the pulse for various separations of the gratings, and creating a plot of both the wavelength and distance. Throughout this report, we demonstrate how one can measure and use a D scan to characterize a pulse, but mainly we determine both theoretically and experimentally the required grating parameters (angle and distance between the gratings) to optimally compress the pulse, achieving the shortest pulse possible for a giving chirped pulse.

1 Experimental Set Up

1.1 Vulcan Petawatt laser

In order to demonstrate our experiment we used the seed of the Vulcan laser system. The Vulcan Petawatt is a 400J, 400 fs Nd:Glass chain laser [7, 8], which can produce laser pulses with intensities up to the order of $\sim 10^{21}\mathrm{Wcm}^{-2}$.

The initial pulse, or 'seed' pulse starts in a hard aperture commercial mode-locked Ti:sapphire laser [9, 10] in the Front End (FE) of Vulcan. It is then divided in two, 90% of it gets amplified in a Nd:YLF regenerative amplifier up to a mJ, while the second part is stretched to 3 ps [11]. The output of the regenerative amplifier (RGA) in the front end is used as an OPCPA pump for the stretched seed, and amplifies the seed using nonlinear methods. Outside the pump duration any background noise of the seed will not be amplified, significantly increasing the contrast of the output pulse [12, 13]. The pulse is then stretched from 3 ps to 4.5 ns in a long Offner stretcher [14]. It is further amplified in a nanosecond OPCPA configuration [15]. This consists of superimposing the seed with a temporary shaped nanosecond pulse [16]. This significantly reduces gain narrowing and provides a method of shaping the pulse spectrum [16, 17]. This stretched pulse is further amplified through a series of disc and rod chains. The amplified pulse is then compressed to short pulse durations, creating a high power pulse on the Petawatt level.

Our focus is on the seed because this is where the majority of the amplification occurs, six orders of magnitude compared to five in the amplification chain. It is this part of the system that plays the most important role in determining the final characteristics of the system, contrast, pulse duration/spectrum, B integral among other effects [11, 18]. In order to analyse the seed, we have inserted a test compressor, which compresses the pulse in parallel to the main Petawatt beam line without introducing significant changes to the Vulcan FE [19]. In particular, the output beam of the nanosecond OPCPA system is now split equally between Vulcan and the new test compressor. As a result, it has been possible to continuously monitor and characterize the Petawatt seed.

1.2 Test Compressor Set Up

The test compressor configuration which is in the FE of Vulcan is shown in Fig. 1 and is used throughout this report to obtain our experimental results. To optimise the test compressor, we measure the spectral intensity of the

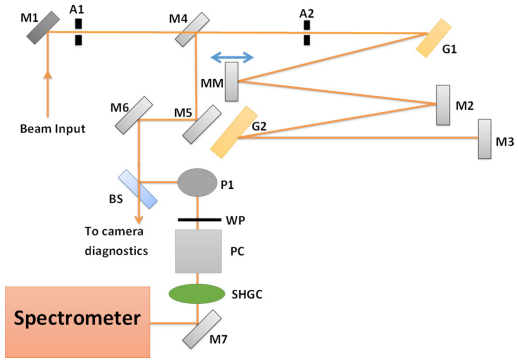

Figure 1: Schematic of the compressor table showing the input beam hitting mirror M1, passing through apertures A1 and A2 onto the compressor gratings (G1 and G2). A periscope (P1), wave-plate (WP), polariser cube (PC), second harmonic generation crystal (SHGC) were placed before the spectrometer. Changing the position of motorised mirror MM changes the dispersion of the pulse by changing the path length. The pulse then travels throughout the set up again, hitting M4 and then is then measured using a spectrometer.

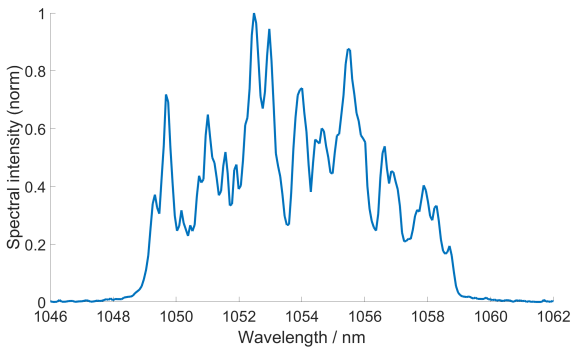

Figure 2: Fundamental spectrum of laser pulse after compression.

second harmonic (SH), a pulse with double the frequency of the initial laser. A second harmonic generation (SHG) crystal and spectrometer were placed at the output of the compressor. After optimising the SHG from the crystal with an IR $\lambda = 1055.5$nm beam, the position of the motorised mirror (MM on Fig.1) stage was changed in small steps whereupon the SH spectrum was recorded for each position. Due to the double pass setup of the compressor, a change in motor position corresponds to quadrupling of the path length through the system allowing a large range of path lengths to be scanned. The compressor was originally designed to have maximum compression with grating distance L = 13 m and grating angle $\gamma = 48.7^o$, resembling the final compressor. We try to replicate the same optical characteristics for this compressor, which has 48.7° incidence angle and 3.25 m in between the gratings in a four pass configuration. This is then folded in three, as seen in 1. The minimum pulse duration is obtained by changing the distance and the angle between the gratings to give optimal compression. We then did five scans at different angles in order to evaluate the pulse duration of the optimally compressed pulse.

2 Theory

2.1 Relationship between Spectral phase and D scans

The spectrum (Fig.2) has a bandwidth of 10nm and has a smooth spectral phase, which can be observed from the lack of complex features on the D scan.

Because of this, we will use the classical Taylor expansion about the central frequency of the pulse [20]. Hence the spectral phase can be written as:

$$\phi(\omega) = \phi_0 + \phi_1(\omega-\omega_0) + \frac{1}{2}\phi_2(\omega-\omega_0)^2 + \frac{1}{6}\phi_3(\omega-\omega_0)^3 ... \tag{1}$$

where ω is the angular frequency, ω_0 is the central frequency and ϕ_n refers to the derivative order of the phase with respect to ω. Each term introduces different effects to the pulse. The first term can be interpreted as a phase shift of the entire pulse to a reference similar to the pulse envelope whereas the second term is simply a shift in the central frequency. Hence, we will be particularly interested in the second and third order terms which physically represent the group delay dispersion (GDD) and the third order dispersion (TOD). GDD enlarges the pulse symmetrically and determines the pulse duration while TOD creates pre- or post-pulses depending on the signal of its term.

The main source of dispersion is given by gratings, both in the two stretchers and the compressor. These gratings represent a geometrical dispersion given by:

$$\phi(\omega, L) = \frac{\omega}{c}\frac{L}{\cos(\gamma)}\cos(\gamma - \alpha(\omega)) \tag{2}$$

where c is the speed of light, L is the distance between the dispersive elements, γ is the angle of incidence of the light as it strikes the grating and α is the angle of the outgoing wave which is frequency dependent.

The D scan signal, which is the intensity of the second harmonic can then be represented by:

$$D(\omega, L) = \mid \sqrt{S(\omega)}\exp i\phi(\omega)W(\omega) \mid^2 \tag{3}$$

where $S(\omega)$ is the signal from the spectrometer as a function of frequency, and $W(\omega)$ is a weight function that is dependent on the spectral acceptance of the second harmonic measured. Due to the small bandwidth (10nm) and the thickness of the crystal (< 0.1mm). We consider this to be constant in this report. By plotting this signal against both wavelength and a distance given by

the alteration to the beam path length we obtain a dispersion scan. Making use of the above, a trial D scan can be created using only the spectrum of the fundamental beam.

We then study the effect of both the GDD and the TOD of a given pulse on the D scan trace itself. To do this, we take the fundamental spectrum of the pulse we measured, and input several values of GDD to the phase as represented in Eq. 1 (all the other coefficients to be zero). These results can be viewed in Fig. 3. From this, we can see that the GDD shifts the displacement of the pulse in the vertical direction.

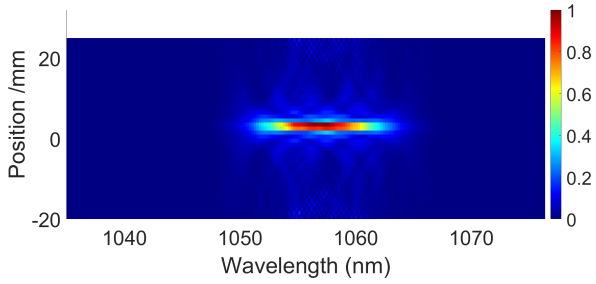

(a) GDD $= 5 \times 10^6 fs^2$

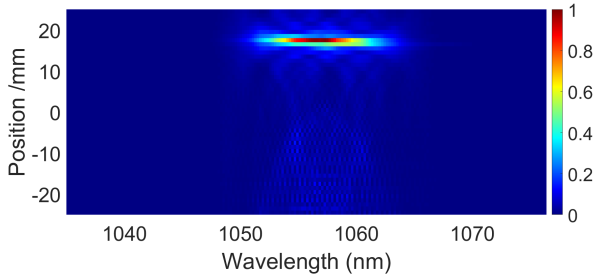

(b) GDD $= -5 \times 10^6 fs^2$

Figure 3: Two Examples of a D scan where the phase only contains GDD

Repeating this for the third order derivative or TOD, one can see that the slope of the maximum values on the D scan change, as seen in Fig 4. Between the highest and the lowest order in Fig. 4 there is a slight slope change, this is due to the residual TOD of the scanned dispersion.

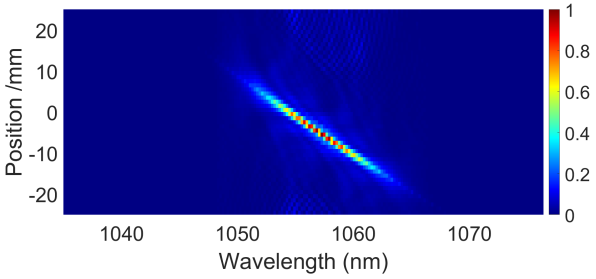

(a) $\phi_3 = -2.3 \times 10^{11} fs^4$

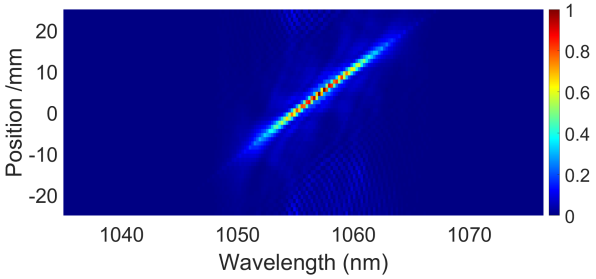

(b) $\phi_3 = 3 \times 10^{14} fs^5$

Figure 4: Two Examples of a D scan where the phase only contains TOD

Higher order derivatives affect the curvature of the maximum values. This can be seen in Figure 5, where the fourth order derivative is scanned through a range of values, creating a quadratic function for the D scan maximum. Similarly, the fifth order derivative is scanned through a range of values creating a cubic function for the maximum of the D scan.

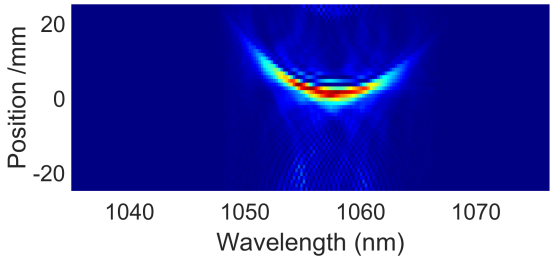

(a) $\phi_4 = -2.3 \times 10^8 fs^3$

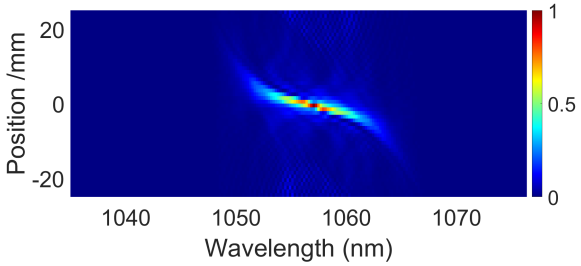

(b) $\phi_5 = 3 \times 10^8 fs^3$

Figure 5: Reconstruction of D scan for higher order derivatives of the phase

In conclusion, the addition of a certain Taylor spectral phase of order n, will create a feature in the D scan which is a polynomial of order $n-2$. From this, GDD will be a constant, TOD a linear curve, fourth order dispersion (FOD), a parabola and so on.

2.2 Algorithm Implementation

Using the fundamental spectrum of the pulse as a trial spectrum, one can introduce a phase, and measure the corresponding D scan. GDD was initially introduced with all other terms in 6 equating to zero. The position of the spectrum was then measured for various different D scans and a calibration curve is plotted in Figure 6. This was then repeated for TOD and another calibration curve was plotted of the TOD as a function of the slope of the D scan, as seen in Figure 7

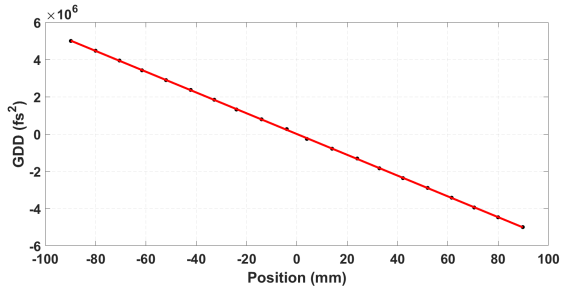

Figure 6: Calibration Curve for the GDD and position,

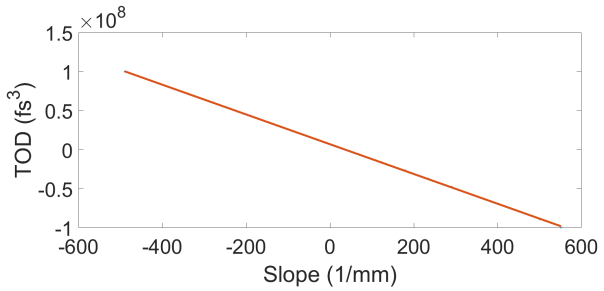

Figure 7: Calibration Curve for the TOD and slope

The above relationships can be given by the following formulae:

$$GDD = (-5.6 \times 10^4)\text{Position} + (3.6 \times 10^{-11}) \quad (4)$$

$$TOD = (-2.0 \times 10^5)\text{Slope} - (1.3 \times 10^{-7}) \quad (5)$$

Using these relationship, one can determine the phase from the position and shape of the experimental data. After obtaining these coefficients (i.e. GDD_0 and TOD_0), the initial values can be determined and a relationship between the TOD and GDD of the pulse can be created to determine the phase for an optimally compressed pulse, as described below.

2.3 Determining the Required Parameters of the Gratings for Optimal Compression

We define the function $f(\gamma, D)$ to be a function which describes the added phase due to the gratings, given in Eq.2. We will also define $D = D_0 + z$, in which D is the absolute distance between gratings, D_0 the nominal distance between gratings (in which the pulse is compressed) and z the difference between the two. Please note that $f(\gamma, D) = f(\gamma, D_0) + f(\gamma, z)$.

This relation gives two degrees of freedom to control the spectral phase. These are the angle of incidence γ and the distance between the two gratings D. These two freedoms contribute to an overall phase allowing the pulse duration to be controlled.

When passing through a pair of gratings the overall phase of the pulse can be described as follows:

$$\Phi = \Phi_0 + f(\gamma, D) \quad (6)$$

where Φ_0 is the initial phase of the pulse and $f(\gamma, D)$ is the additional phase produced by the pair of gratings. We then define ϕ_0 to be the phase of the pulse for maximum compression, as given by: $\phi_0 = \Phi_0 + f(\gamma, D_0)$, which is the actual phase at the output of the compressor. In order to minimise all the phase terms, we require the overall phase to be constant, or the group delay to be zero. If GDD and TOD introduced by the gratings are the second and third order derivatives of the function f, from [21] they can then be viewed as;

$$f_n(\gamma, \omega, D) = C_n(\gamma, \omega)D \quad (7)$$

for $n = 2, 3...$, where:

$$C_2(\gamma, \omega) = \frac{-4\pi^2 c}{w^3 d^2 \cos^3(\alpha)} \quad (8a)$$

$$C_3(\gamma, \omega) = \frac{12\pi^2 c}{\omega^4 d^2 \cos^3(\alpha)}(1 + \frac{2\pi c sin(\alpha)}{\omega d \cos^2(\alpha)}) \quad (8b)$$

With this we can expand these two terms (f_2 and f_3) to the first order on both D and γ to evaluate what small changes could do to the additional phase. These small changes are denoted by Δf and are given by:

$$\Delta f_n = C_n(\gamma, \omega)z + C'_n(\gamma, \omega)D\Delta\gamma, n = 2 \text{ and } 3 \quad (9)$$

In which $C'_n(\gamma, \omega)$ is the derivative in relation to γ. These derivatives were found to be

$$C'_2 = -\frac{12\pi^2 c \sin\alpha \cos\gamma}{w^3 d^2 \cos^5(\alpha)} \quad (10a)$$

$$C'_3 = \frac{12\pi^2 c \cos\gamma}{\omega^4 d^2 \cos^5(\alpha)}(3\sin\alpha + \frac{2\pi c}{\omega d}\{\frac{5}{\cos^2\alpha} - 4\}) \quad (10b)$$

In every D-scan trace we will be changing the distance between the gratings while keeping the angle constant, we can say that the TOD and the GDD of the pulse itself that are the second and third derivatives of ϕ_0 as given above can be given by:

$$GDD = GDD_0 + C_2(\gamma, \omega_0).z \tag{11a}$$

$$TOD = TOD_0 + C_3(\gamma, \omega_0).z \tag{11b}$$

In which GDD_0 and TOD_0 are initial conditions that have not been compressed. Please note that we could establish a linear relation between the variation of TOD and GDD, which can be translated in:

$$TOD = \frac{C_3}{C_2}.GDD + (TOD_0 - \frac{C_3}{C_2}GDD_0) \tag{12}$$

The above equations are only valid for a given D scan, where the angle of the gratings is kept constant. To minimize TOD when GDD is equals zero we will have change both the angle and the distance. The variation of the phase introduced by the compressor that is given in Eq.9 has to be $\Delta f_3 = -TOD_0$ while GDD stays the same $\Delta f_2 = 0$. In this case the change in angle is given by Eq.13.

$$\Delta\gamma = \frac{-TOD_0.C_2(\gamma, \omega_0)}{D.(C_2(\gamma, \omega_0)C_3'(\gamma, \omega_0) - C_3(\gamma, \omega_0)C_2'(\gamma, \omega_0))} \tag{13}$$

The distance between the grating would have to change as well by:

$$z = -\frac{D}{C_2(\gamma, \omega_0)}C_2'(\gamma, \omega_0)\Delta\gamma \tag{14}$$

From here, it is obvious that to compress the pulse, one must change both the angle and the distance between the gratings. We can combine this and the calibration obtained in Eqn 4 to determine how much we need to move the gratings to get the TOD to zero.

Results

Five D scans were carried out for various angles between the gratings, ranging from 48 degrees to 49.7 degrees. These D scans can be seen below in Fig. 10 in the Appendix.

Analysis and discussion

In order to obtain the GDD and TOD of the pulse measured for each D scan, we used the calibration given in Fig.6 and Fig.7.

Here the position of the trace is dependant on the GDD, while the slope, represented by the green line in each figure is dependant on the TOD. In order to determine the curvature of the compressed pulse in the

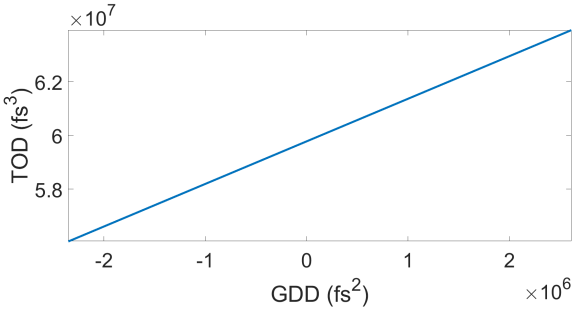

Figure 8: Theoretical results of the linear relation between GDD and TOD over the 25mm of scan. Values calculated for the measurement done with an incident angle of 48.7 degrees.

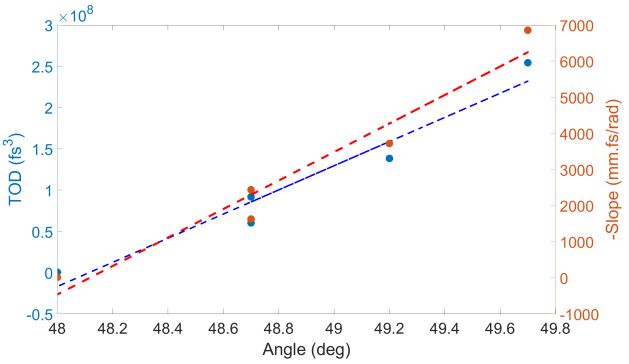

Figure 9: Experimental results of TOD (blue) and slope (red) of the D-scan trace as a function of the angle.

experimental data, higher order terms of the Taylor Expansion would need to be calculated. However, as we are just interested in tuning the compressor and hence the GDD and TOD here, only the phase up to the third order of the Taylor Expansion is needed.

The measured D scan can be seen on the left of each figure, and its reconstruction on the right of each figure, up to the third order of its phase (TOD). By determining the position and slope of the maximum intensities in each D scan, one can use these calibration curves to determine the GDD, TOD and phase of the angle.

For the angle of 48.7 degrees we calculated the theoretical TOD/GDD relation, as it is giving in Eq.12. This relationship can be seen in Fig.8

Fitting a linear relationship between the angle γ and TOD using equation 12, one obtains a slope of 1.53×10^8 fs^3/deg for a nominal angle of incidence of 48.7 degrees. This was repeated for an incident angle of 49 degrees and the slope of this relation was found to be 1.44×10^8 fs^3/deg, using Eqn 13.

From our experimental data, one also obtains a relationship between TOD and angle, with a slope of 1.46×10^8 fs^3/deg with an uncertainty of $2.0 \times 10^{-}7$ fs^3/deg.

Comparing both the theoretical and experimental slopes of this linear fit, one can see they are in agreement with

one another. From this we can confirm our theoretical analysis of the relationship between D scans and phase. We can therefore use equation 13 and equation 14 to calculate the parameters required to optimally compress the pulse for a given grating pair.

Conclusions

We can conclude that D scan is an easy to use method of phase reconstruction that is appropriate to tune the characteristics of a compressor to minimize the pulse duration and maximise the output intensity of the laser at Vulcan. While doing so, we have presented an analytical expression to do it and confirmed it experimentally. Using these parameters for the grating compressors at Vulcan, we can thus compress the pulse to its shortest pulse duration.

References

[1] P. Boller, A. Zylstra, P. Neumayer, L. Bernstein, C. Brabetz, J. Despotopulos, J. Glorius, J. Hellmund, E. A. Henry, J. Hornung, J. Jeet, J. Khuyagbaatar, L. Lens, S. Roeder, T. Stoehlker, A. Yakushev, Y. A. Litvinov, D. Shaughnessy, V. Bagnoud, T. Kuehl, and D. H. G. Schneider, "First on-line detection of radioactive fission isotopes produced by laser-accelerated protons," *Scientific Reports*, vol. 10, p. 17183, Oct 2020.

[2] F. Pressacco, V. Uhlíř, M. Gatti, A. Nicolaou, A. Bendounan, J. A. Arregi, S. K. K. Patel, E. E. Fullerton, D. Krizmancic, and F. Sirotti, "Laser induced phase transition in epitaxial ferh layers studied by pump-probe valence band photoemission," *Structural Dynamics*, vol. 5, no. 3, p. 034501, 2018.

[3] Z.-H. Loh and S. R. Leone, "Capturing ultrafast quantum dynamics with femtosecond and attosecond x-ray core-level absorption spectroscopy," *The Journal of Physical Chemistry Letters*, vol. 4, no. 2, pp. 292–302, 2013. PMID: 26283437.

[4] K. Sugioka and Y. Cheng, "Ultrafast lasers—reliable tools for advanced materials processing," *Light: Science & Applications*, vol. 3, pp. e149–e149, Apr 2014.

[5] H. Ueba and B. Gumhalter, "Theory of two-photon photoemission spectroscopy of surfaces," *Progress in Surface Science*, vol. 82, no. 4, pp. 193–223, 2007. Dynamics of Electron Transfer Processes at Surfaces.

[6] T. Miranda, M.and Fordell, C. Arnold, A. L'Huillier, and H. Crespo, "Simultaneous compression and characterization of ultrashort laser pulses using chirped mirrors and glass wedges," *Opt. Express*, vol. 20, pp. 688–697, Jan 2012.

[7] C. Danson, P. Brummitt, R. Clarke, J. Collier, B. Fell, A. Frackiewicz, S. Hancock, S. Hawkes, C. Hernandez-Gomez, P. Holligan, M. Hutchinson, A. Kidd, W. Lester, I. Musgrave, D. Neely, D. Neville, P. Norreys, D. Pepler, C. Reason, W. Shaikh, T. Winstone, R. Wyatt, and B. Wyborn, "Vulcan petawatt—an ultra-high-intensity interaction facility," *Nuclear Fusion*, vol. 44, pp. S239–S246, nov 2004.

[8] C. Hernandez-Gomez, P. Brummitt, D. Canny, R. Clarke, J. Collier, C. Danson, A. Dunne, B. Fell, A. Frackiewicz, S. Hancock, S. Hawkes, R. Heathcote, P. Holligan, M. Hutchinson, A. Kidd, W. Lester, I. Musgrave, D. Neely, D. Neville, and B. Wyborn, "Vulcan petawatt-operation and development," *Journal de Physique IV (Proceedings)*, vol. 133, 06 2006.

[9] D. E. Spence, P. N. Kean, and W. Sibbett, "60-fsec pulse generation from a self-mode-locked ti:sapphire laser," *Opt. Lett.*, vol. 16, pp. 42–44, Jan 1991.

[10] N. H. Rizvi, P. M. W. French, and J. R. Taylor, "Continuously self-mode-locked ti:sapphire laser that produces sub-50-fs pulses," *Opt. Lett.*, vol. 17, pp. 279–281, Feb 1992.

[11] I. Musgrave, W. Shaikh, M. Galimberti, A. Boyle, C. Hernandez-Gomez, K. Lancaster, and R. Heathcote, "Picosecond optical parametric chirped pulse amplifier as a preamplifier to generate high-energy seed pulses for contrast enhancement," *Appl. Opt.*, vol. 49, pp. 6558–6562, Nov 2010.

[12] A. Dubietis, G. Jonušauskas, and A. Piskarskas, "Powerful femtosecond pulse generation by chirped and stretched pulse parametric amplification in bbo crystal," *Optics Communications*, vol. 88, no. 4, pp. 437–440, 1992.

[13] I. Ross, P. Matousek, M. Towrie, A. Langley, and J. Collier, "The prospects for ultrashort pulse duration and ultrahigh intensity using optical parametric chirped pulse amplifiers," *Optics Communications*, vol. 144, no. 1, pp. 125–133, 1997.

[14] G. Cheriaux, P. Rousseau, F. Salin, J. P. Chambaret, B. Walker, and L. F. Dimauro, "Aberration-free stretcher design for ultrashort-pulse amplification," *Opt. Lett.*, vol. 21, pp. 414–416, Mar 1996.

[15] C. Hernandez-Gomez, P.A. Brummitt, D.J. Canny, R.J. Clarke, J. Collier, C.N. Danson, A.M. Dunne, B. Fell, A.J. Frackiewicz, S. Hancock, S. Hawkes, R. Heathcote, P. Holligan, M.H.R. Hutchinson, A. Kidd, W.J. Lester, I.O. Musgrave, D. Neely, D.R.

Neville, P.A. Norreys, D.A. Pepler, C.J. Reason, W. Shaikh, T.B. Winstone, and B.E. Wyborn, "Vulcan petawatt-operation and development," *J. Phys. IV France*, vol. 133, pp. 555–559, 2006.

[16] P. Oliveira, S. Addis, J. Gay, K. Ertel, M. Galimberti, and I. Musgrave, "Control of temporal shape of nanosecond long lasers using feedback loops," *Opt. Express*, vol. 27, pp. 6607–6617, Mar 2019.

[17] F. Batysta, R. Antipenkov, T. Borger, A. Kissinger, J. T. Green, R. Kananavičius, G. Chériaux, D. Hidinger, J. Kolenda, E. Gaul, B. Rus, and T. Ditmire, "Spectral pulse shaping of a 5 hz, multi-joule, broadband optical parametric chirped pulse amplification frontend for a 10 pw laser system," *Opt. Lett.*, vol. 43, pp. 3866–3869, Aug 2018.

[18] B. Parry, P. Oliveira, A. Boyle, W. Shaikh, and I. Musgrave, "A new ns opcpa front end for vulcan petawatt," *CLF Annual Report*, 2013.

[19] A. S. Wyatt, H. Owen, P. Oliveira, B. Parry, M. Galimberti, and I. Musgrave, "Design and implementation of a test compressor for the vulcan front end," *CLF Annual Report*, no. 34, 2017.

[20] L. G. Cohen and C. Lin, "Pulse delay measurements in the zero material dispersion wavelength region for optical fibers," *Appl. Opt.*, vol. 16, pp. 3136–3139, Dec 1977.

[21] I. Walmsley, L. Waxer, and C. Dorrer, "The role of dispersion in ultrafast optics," *Review of Scientific Instruments*, vol. 72, no. 1, pp. 1–29, 2001.

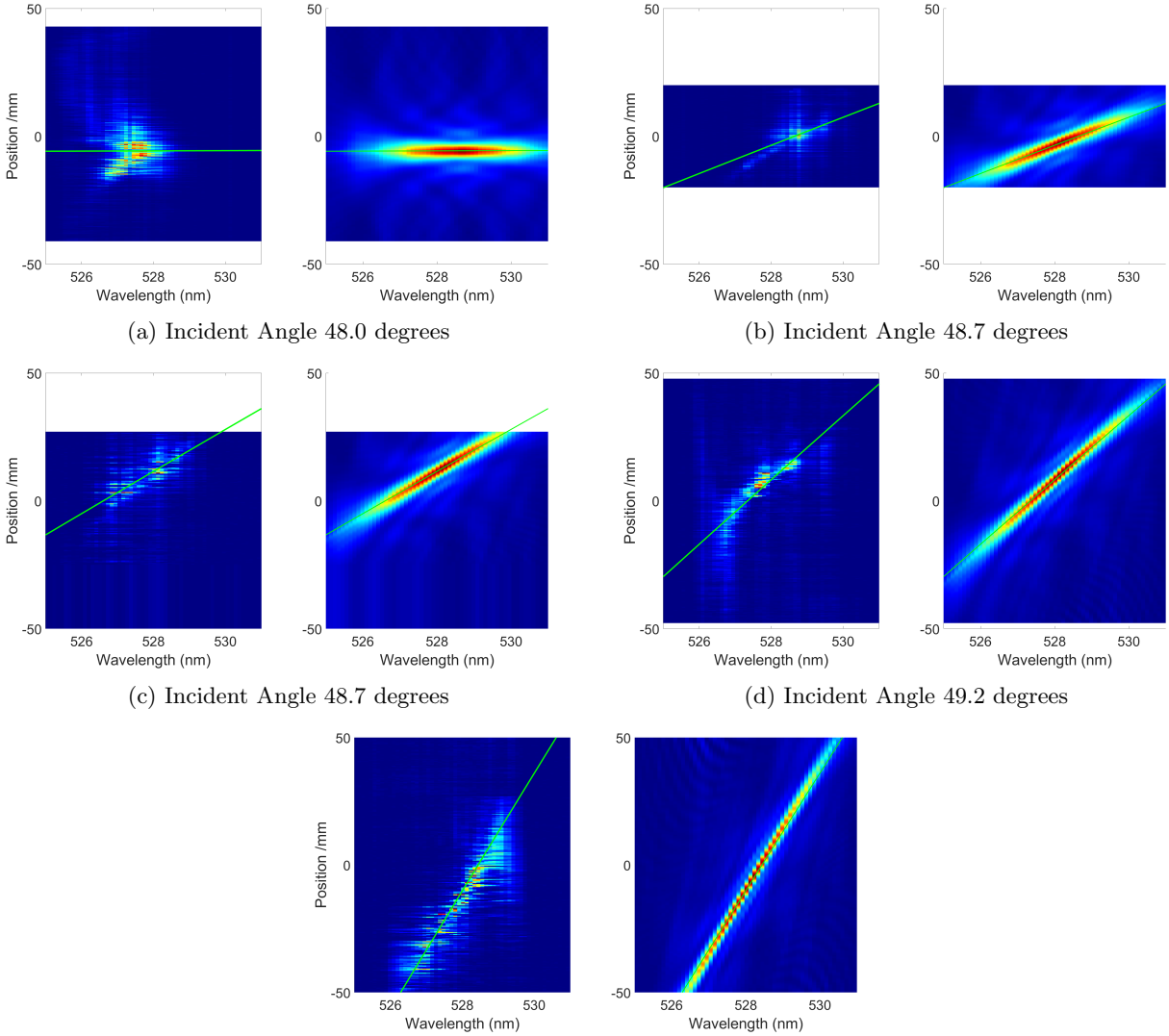

(a) Incident Angle 48.0 degrees

(b) Incident Angle 48.7 degrees

(c) Incident Angle 48.7 degrees

(d) Incident Angle 49.2 degrees

(e) Incident Angle 49.7 degrees

Figure 10: Examples of Dispersion Scans, each with different incident angles (on the left), and their reconstructions up using a reconstruction of the phase up to third order (on the right).